Frontal ridge slope failure at the northern Cascadia margin: Margin-normal fault and gas hydrate control

Caroll López[1], George Spence[1], Roy Hyndman[1,2], and Deborah Kelley[3]
[1]School of Earth and Ocean Sciences, University of Victoria, Victoria, BC V8W 3V6, Canada
[2]Geological Survey of Canada–Pacific, 9860 W. Saanich Road, Sidney, BC V8L 4B2, Canada
[3]School of Oceanography, University of Washington, Seattle, Washington 98195, USA

ABSTRACT

On the northern Cascadia accretionary margin off Vancouver Island, Canada, there are numerous sedimentary slide features near the base of the slope, and significant amounts of gas hydrate found beneath the ridge suggest a possible connection. A 2-km-wide collapse structure with a 300-m-high headwall has been studied by multibeam bathymetry and a single-channel seismic reflection grid. Migrated seismic reflection lines on the frontal ridge image multiple 15–75-m-high seafloor scarps perpendicular to the margin that are the seafloor expressions of normal faults that cut deeply into the sediment section. Two of the largest faults are aligned with the sidewalls of the slide, indicating that the lateral extent of the collapse is fault controlled. The presence of marine gas hydrate beneath the ridge is based on a widespread hydrate bottom-simulating reflector (BSR), high velocities determined by ocean bottom seismograph data, and sediment core samples and downhole logs collected by the Integrated Ocean Drilling Program at Site U1326. The depth of the BSR at 255 (±15) m coincides closely with the estimated depth of the glide plane beneath the slide. This suggests that the base of the slope failure is related to the contrast between strong hydrate-cemented sediments above the BSR and underlying weak sediments containing free gas. Strong earthquake shaking on this convergent margin likely provides the trigger for the slide.

INTRODUCTION

Submarine landslides on continental slopes are important geologic hazards for seafloor facilities, such as communication cables and infrastructure for hydrocarbon exploration. It has been suggested that in regions containing gas hydrates, slides may result in a rapid release of methane that contributes to global warming (Pecher et al., 2005; Mienert et al., 2005). The larger slides may generate tsunamis that can cause substantial coastal damage and human hazard. For example, 2200 lives were lost in the A.D. 1998 tsunami associated with the magnitude 7.1 Papua New Guinea earthquake; the tsunami was likely produced by the seafloor slide that was triggered by the earthquake (Synolakis et al., 2002).

Numerous studies have suggested a direct link between slope failure and the presence of gas hydrate, but the issue is controversial. Possible examples are found on the eastern Canada margin (Mosher, 2009), on the United States Atlantic continental slope (Hornbach et al., 2007), and at the Storegga slide on the Norwegian margin (Berndt et al., 2005a). The dissociation of gas hydrate may (1) provide a zone of weakness at the bottom-simulating reflector (BSR) that localizes the glide plane (Dillon et al., 1998), or (2) cause sediment liquefaction during or immediately after a slide event (Berndt et al., 2005b). In contrast, at the Storegga slide, Brown et al. (2006) found that the base of hydrate stability was deeper than the glide plane at the time of slope failure, and hence do not consider gas hydrate dissociation as a primary cause of slide initiation. Alternative mechanisms, such as contrasting geotechnical properties between sediments deposited in glacial and interglacial times, have been suggested (Solheim et al., 2005).

On the seismogenic Cascadia margin off Vancouver Island, a number of large slope failures have been identified on the frontal anticlinal ridges and there is a wide distribution of gas hydrates. In this paper we describe one of the frontal ridge slides, located near Site U1326 of the Integrated Ocean Drilling Program (IODP). We present evidence from swath bathymetry, seismic reflection, and ocean bottom seismic refraction data to show that the failure glide plane occurred at the same depth as the base of gas hydrate stability, and that the lateral limits of the slide are controlled by margin-perpendicular normal faults.

DATA COLLECTION AND PROCESSING

This study is based mainly on sea-surface EM 300 multibeam bathymetry data, collected in 2004 during University of Washington cruise TN175, on single-channel seismic (SCS) data from Geological Survey of Canada cruise PGC0408 (Fig. 1), and on results from IODP Site 1326. Processing of SCS lines included gap deconvolution and finite difference time migration, with velocities based on the Site 1326 sonic log. The migration was successful in collapsing seafloor diffractions to a series of sharp seafloor scarps, with offsets as large as 65 m (Fig. 2). The larger ridges and troughs are also seen clearly in the swath bathymetry data, both in map view (Fig. 1) and in depth profiles perpendicular to the scarps (Fig. 3A).

Seismic structure beneath the ridge, including layer velocities and thicknesses, was determined from a wide-angle reflection and refraction survey using a grid of 8 ocean bottom seismometers (OBS), collected in 2005 during cruise PGC0509 (López, 2008; see the GSA Data Repository[1] for details on data collection and analysis, and Figs. DR1–DR3 therein).

During cruise PGC0809 in 2008, piston cores were taken across the target slide and a slide on a neighboring frontal ridge segment (Pohlman et al., 2008). The cores sampled the headwall, the glide plane, and the slide deposits. IODP Site 1326 penetrated the top of the frontal ridge near the headwall, providing sediment analyses and downhole geophysical data that define gas hydrate concentrations to the depth of the BSR at 255 m (Riedel et al., 2006).

SLIDE DESCRIPTION AND TIMING

The 2-km-wide slope failure is located on the seaward side of the frontal ridge in the middle part of the local ridge structure (Fig.1). The slide structure covers an area of ~3.5 km^2. The slide headwall is ~300 m high, with an average slope of ~30º. The seaward mouth of the collapse is <1 km wide, suggesting that later stage collapses have occurred and eroded further into the frontal ridge.

Sedimentological analyses of piston cores show that the slumped material includes glaciomarine sediments with diagenetically altered black clays, similar to shallow stratigraphy above the headwall. Thus, the age of the slide likely postdates Wisconsinan deglacial deposits (ca. 14 ka). In one core, a succession of 10 turbidites and hemipelagic clays overlies the failure deposits, suggesting that the slide is several thousand years old, assuming that they are caused by major earthquakes every 500–700 yr (Goldfinger et al., 2003). For a neighboring slide

[1]GSA Data Repository item 2010270, wide-angle traveltime analyses, refraction velocity models, and additional single-channel seismic record sections, is available online at www.geosociety.org/pubs/ft2010.htm, or on request from editing@geosociety.org or Documents Secretary, GSA, P.O. Box 9140, Boulder, CO 80301, USA.

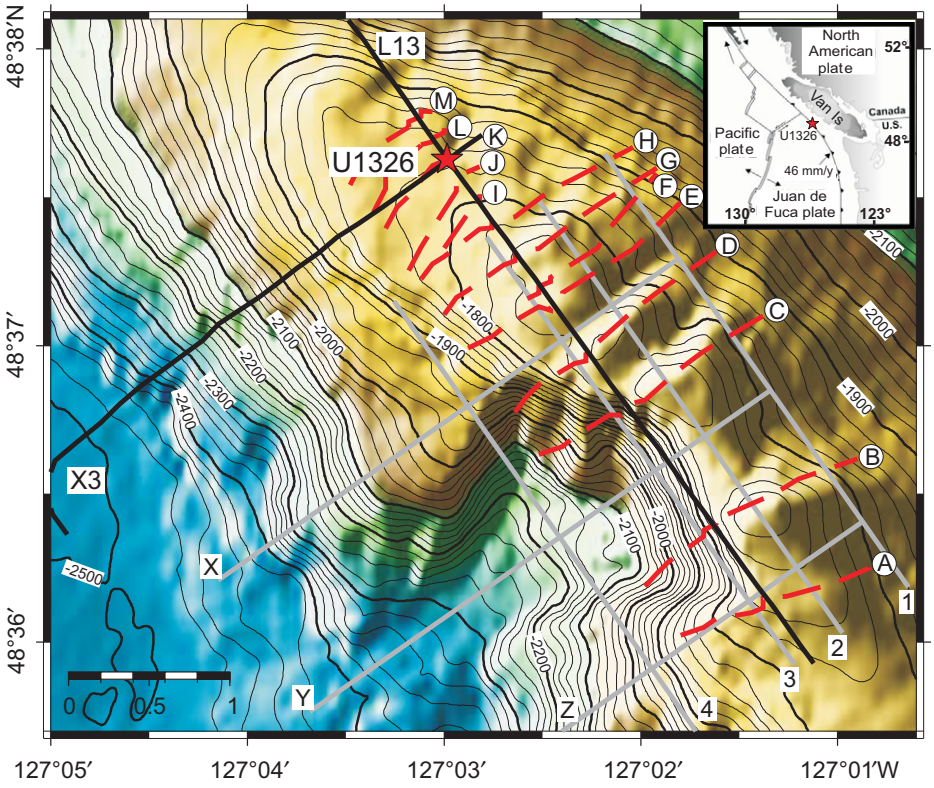

Figure 1. Swath bathymetric map of frontal ridge segment off Vancouver Island. Inset shows tectonic setting, with convergence at 46 mm/yr. Seismic lines L13 and X3 (black lines) are shown in Figure 2A. Labeled red dashed lines correspond to peaks of seafloor scarps identified on grid of single-channel seismic lines and also seen in seafloor bathymetry. Scarps B and D align with main sidewalls of slide; scarps A and C may represent subsequent slide event that cut further into ridge. Red star is Site U1326 of the Integrated Ocean Drilling Program X311. Depths from bathymetric profiles 1, 2, 3, 4, X, Y, and Z (gray lines) are shown in Figure 3. Contour interval is 20 m.

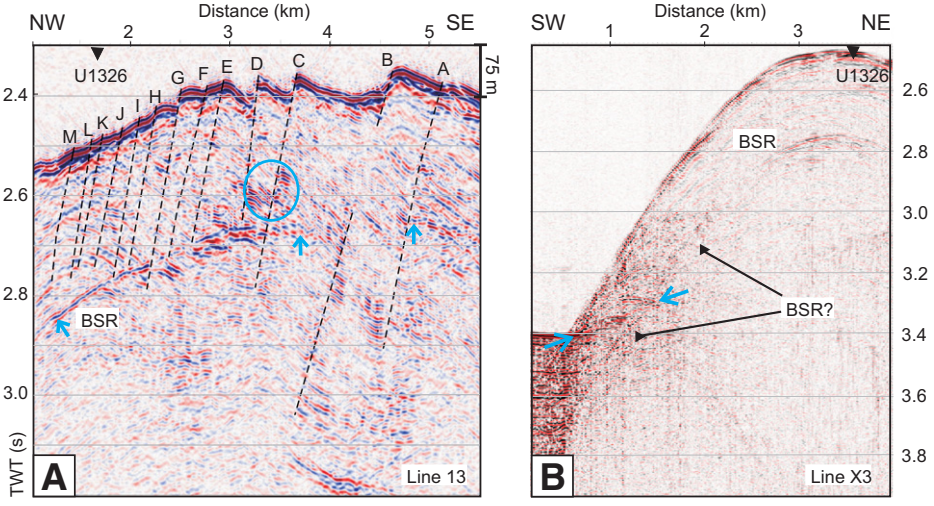

Figure 2. Migrated seismic lines (see Fig. 1 for location). TWT—two-way traveltime. A: Line L13 shows prominent seafloor scarps. These are associated with normal faults identified by reflector terminations and offsets. Faults are likely produced by longitudinal flexure associated with central uplift of ridge segment. Bottom-simulating reflector (BSR) is located ~275 ms below seafloor at top of ridge. B: On line X3, subtle BSR seen beneath slope crosscuts lithology at ~290 m below seafloor near base of slope. Blue arrows on line X3 indicate possible fault or lithological surface connecting seafloor to BSR; surface could be future failure plane along which slide initiates before cutting to depth of BSR.

just to the southeast, a minimum age of 5000 yr is estimated from geochemical modeling of the time required to reestablish the sulfate gradient in material beneath the glide plane (Pohlman et al., 2008).

EVIDENCE FOR GAS HYDRATE BENEATH RIDGE

There is strong evidence that gas hydrate is widely distributed beneath the ridge.

(1) A BSR is easily identified over much of the region surrounding the slide (Fig. 2), especially near the crest of the ridge and to the northwest of the slide in a strip ~1 km in width (Fig. DR1). Beneath the headwall and slide deposits, particularly between scarps B and C, there is almost no BSR or other reflectivity in the upper 300–400 ms (Fig. 2; Figs. DR4 and DR5).

(2) At Site U1326 of IODP Expedition X311, hydrate was observed directly and inferred from drilling logs (Riedel et al., 2006). On sonic velocity and resistivity logs, a layer of concentrated hydrate (>50% of pore space) was found at a depth of 72–107 m below the seafloor (mbsf), plus substantial hydrate saturations (20%–25%) in the 70 m interval above the BSR at a depth of 255 (±15) m.

(3) The wide-angle reflection and refraction survey found high seismic velocities above the BSR consistent with the presence of hydrate and extending out to distances of at least 4 km from the drillhole (Fig. DR3). A layer from 80 to 110 mbsf was interpreted to have average concentrations of 30%–35%, and concentrations in the layer above the BSR were also 20%–30% (see the Data Repository).

DESCRIPTION OF FRONTAL RIDGE FAULTS

A set of 13 seafloor scarps, A–M, was identified on the migrated SCS sections. The scarps appear to be seafloor expressions of normal faults that cut through the accreted sediments of the frontal ridge, to depths below the BSR in some locations (e.g., line 13 in Fig. 2A). The seafloor traces of faults were mapped from the SCS data set by picking the high point of the scarps, since there is less uncertainty in this location than in the foot of the scarp. The fault traces were then superimposed on the detailed bathymetry map (Fig. 1). There is a good correlation between the seismically and bathymetrically defined faults where seafloor offsets are large (e.g., faults A–H).

The faults strike northeast-southwest, perpendicular to the margin and parallel to the direction of convergence. The two faults with the largest seafloor scarps, B and C (Fig. 2), bound an interior region of maximum slope failure, whereas faults A and D bound the outer limits of failure and correlate with the sidewalls of the faulted region. Faults I–M, which are less easily

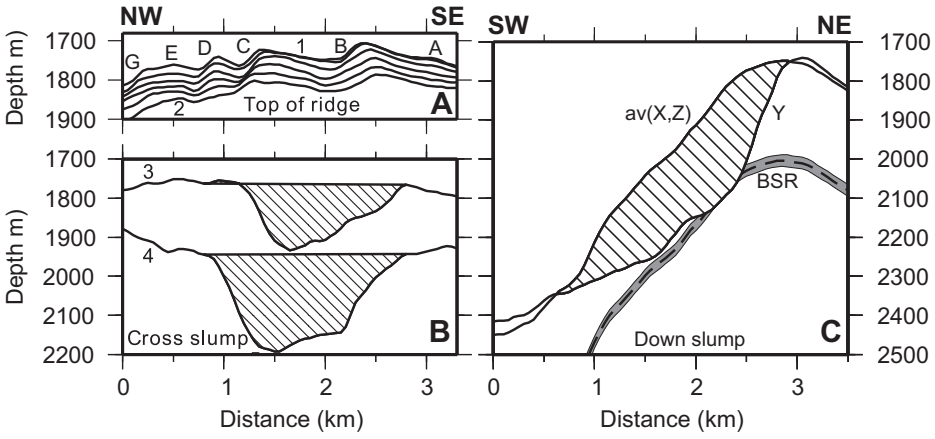

Figure 3. A: Water depths along lines at 200 m spacing between profiles 1 and 2 (Fig. 1). Only seafloor scarps A, B, C, D, E, and G are identifiable in bathymetry of Figure 1. B: Along profiles 3 and 4, original pre-slump surface is estimated by interpolating across slump. C: Present water depths down the slump are shown along profile Y, and pre-slump surface is estimated as average (av) depths along X and Z. Inferred depth of bottom-simulating reflector (BSR) beneath pre-slump surface coincides closely with glide plane; BSR depth error is indicated by gray shading.

identified, appear as subtle features in the SCS seafloor reflection.

NATURE OF FAULTS AND RELATION TO SLIDE

Most of the largest fault scarps, A–H, strike at high angles to the bathymetric contours of the ridge. Thus these faults cannot be simple gravitational sliding features. Rather, they are interpreted as normal faults with fault displacement in the direction of northwest-southeast extension. The strongest evidence of normal faulting is for faults C and D (Fig. 2A), where at ~2.6 s, stratigraphic reflectors are terminated sharply. The terminations are aligned with the seafloor scarps and some displacement is observed. For fault B, reflector terminations aligned with the seafloor scarp are clearer below the BSR.

The lateral extent of slumping is clearly fault controlled, as indicated by the seafloor traces of the primary faults A–D determined from the seismic and bathymetry data (Fig. 1). The primary faults are margin normal, whereas the orientation of the slide headwall is margin parallel. The area of sediment that slumped is thus rectangular at the seafloor. This rectangular pattern of slumps is observed in the swath bathymetry data at many other locations along the northern Cascadia margin (e.g., see Fig. DR1 and Mosher, 2009).

The origin of the margin-normal faults must be related to the stress regime in the sediments and to the processes of sediment ridge formation. The orientation of the ridges is nearly parallel to the deformation front and perpendicular to the direction of maximum compressive stress. Folding and faulting of the incoming ~2.5-km-thick sedimentary section over a detachment near the top of the oceanic plate shortens the overriding accretionary sediment package (Davis and Hyndman, 1989). The frontal ridge is quite segmented, with typical ridge lengths of 10–20 km parallel to the margin. Folding and extension in the central uplift region will most easily be accommodated in the direction of least compressive stress, which is parallel to the ridge orientation. Normal faulting is thus expected with the faults striking perpendicular to the margin. The steepest seafloor slopes are on the seaward side of the frontal ridge, where underthrusting may be localized; slumping occurs on these slopes with a headwall parallel to the margin. The slide headwall is also a normal fault surface that can be considered to form as a means of accommodating uplift and flexural extension.

SLIDE MECHANISMS

Zone of Weakness at Base of Gas Hydrate

On the Vancouver Island frontal ridge, the depth correspondence between the failure glide plane and the base of gas hydrate stability appears to be very good. The depth of the slide detachment was estimated from the detailed swath bathymetry data. A reconstruction of the old ridge, before the slide event, was made by interpolating the predominant trends of the contours along the slope using bathymetry profiles X just to the south of the slump and Z just to the north (Figs. 1 and 3). Current water depths along profile Y through the slide provide an approximation for the failure surface. The mid-slide thickness, beneath profile Y, is ~255 m. The amount of material removed is calculated by finding the volume between the original and final surfaces. The slide volume is ~0.43 km^3. However, slide material likely accumulated above the failure plane and so the current water depth profile is a minimum estimate for the failure plane depth; the calculated volume is thus a minimum estimate. Other nearby slides on the North Cascadia margin have even larger slide dimensions; nevertheless, the volume of ~0.5 km^3 is a sizeable fraction of the estimated 1–4 km^3 slide volume associated with the 1998 tsunamigenic earthquake in Papua New Guinea.

The average BSR depth beneath the upper portion of the ridge is 255 (±15) m from the OBS refraction analyses (López, 2008; see the Data Repository). The limitations of single-channel seismic data collection perpendicular to the ridge and deformation front make it difficult to image reflectors beneath the steep slopes. However, a weak BSR can be identified beneath the lower portion of the ridge on line X3, which passes through IODP Site U1326 (Fig. 2B); its depth increases to ~270 mbsf at the foot of the ridge, consistent with the expected increase in BSR depth with increasing water depth. This provides an estimate for BSR depth beneath the original surface of the slide prior to failure.

As represented by current depths along slide profile Y, the base of the slide coincides with the depth of the nearby BSR for a distance of ~1.0 km (Fig. 3C). The BSR depth is ~30 m greater than the depth of the slide base for the deeper half of this distance range; however, given that the BSR depth error is ±15 m and the current water depth is a minimum estimate for the slide base, the surfaces are coincident within the estimated error. This correspondence provides strong support for the hypothesis that the BSR acted as a glide plane for the slide failure. The sediments above the BSR are cemented by the gas hydrate and thus strengthened; in contrast, the top of the free gas is a zone of weakness, which thus forms the failure surface.

It is unlikely that the failure plane follows a single marine clay layer with strain-softening behavior, as has been modeled quantitatively for the Storegga slide (Kvalstad et al., 2005). Structure and deformation on the frontal ridge are very complex, and (unlike the BSR) stratigraphy at the depth of the failure plane is not parallel to the seafloor over the central part of the steep slope. Thus, except for possibly the toe of the slide (blue arrows in Fig. 2B), the glide plane has cut at high angles through the existing stratigraphy (see also Fig. DR6b along line X7 through the slide).

Earthquakes

The Cascadia subduction zone generates major earthquakes with moment magnitudes as large as Mw = 9 beneath the study site and very strong shaking, at an average interval of ~500 yr (e.g., Hyndman et al., 1996).

A large earthquake is the most likely direct trigger mechanism for the slope failures on the frontal ridge of the Cascadia margin. As

reviewed by Wright and Rathje (2003), mechanisms may include (1) acceleration-induced sliding, (2) steepening of the ground surface profile by motion along the frontal thrust, or (3) reduction in sediment shear strength by induced excess pore water pressures. These factors may be particularly important near the toe of the steep slope, in the region of faults associated with the frontal thrust.

Combined Mechanism

Following Kvalstad et al. (2005), we interpret the slide mechanism as a retrogressive failure in which a series of triangular blocks or wedges progressively cut back from the toe of the slope to the current headwall. The initial failure, triggered by an earthquake, cut through the sediments from the seafloor to a depth of ~260–270 mbsf, possibly following a fault or lithological surface such as indicated along line X3 in Figure 2B. At this depth, we observe that the glide plane was coincident with the depth of the BSR prior to failure, and so we infer that retrogression then followed a zone of weakness that is coincident with the base of the hydrate layer. The earthquake trigger likely increased pore pressures along the faults striking perpendicular to the margin and across the ridge, and reduced shear strength and overall frictional resistance to slide block motion. The lateral extent of failure is thus controlled by these faults.

CONCLUSIONS

A slide structure observed in multibeam bathymetry data and in seismic reflection data at the northern Cascadia frontal ridge is fault controlled. A series of normal faults, striking perpendicular to the ridge and parallel to the direction of tectonic compression, were mapped. They are associated with large well-imaged 25–75-m-high seafloor scarps. The region of slope failure is bounded by two of the major faults. The faults are likely related to the three-dimensional nature of the ~12-km-long ridge uplift, i.e., formed by flexure-associated motion in a direction parallel to the direction of least compressive stress. This pattern of margin-normal faulting adds complexity to the deformation in frontal ridge regions.

With widespread hydrate beneath the ridge, the estimated depth of the slide detachment or glide plane coincides closely with the BSR depth, which is well constrained by OBS seismic refraction data. This strongly suggests that the depth of the failure surface in this area is controlled by the base of gas hydrate. Free gas weakens the sediments beneath the BSR relative to those above the BSR, and so the BSR acts as a basal detachment surface. High fluid flux and high pore pressures along the margin-normal faults may further weaken the sediments within the faults, and enable the largest of these faults to act as the sidewall detachment surfaces for the slide. The actual trigger for the slide failure is likely strong earthquake shaking on this subduction margin.

ACKNOWLEDGMENTS

We thank Bob Macdonald and Ivan Frydecky for their technical expertise in ship operations. This work was supported by grants from the Natural Science and Engineering Research Council and by ship time from the Canadian Department of Fisheries and Oceans. We acknowledge Seismic Micro-Technology for the use of KINGDOM software. Geological Survey of Canada publication 20080292.

REFERENCES CITED

Berndt, C., Mienert, J., Vanneste, M., and Bünz, S., 2005a, Gas hydrate dissociation and sea floor collapse in the wake of the Storegga Slide, Norway, *in* Wandås, B.T.G., et al., eds., Onshore-offshore relationships on the North Atlantic Margin: Proceedings of a conference held in Trondheim, 2002: Norwegian Petroleum Society (NPF) Special Publication 12: Amsterdam, Elsevier, p. 285–292.

Berndt, C., Mienert, J., Vanneste, M., Bunz, S., and Bryn, S., 2005b, Submarine slope-failure offshore Norway triggers rapid gas hydrate decomposition, *in* Wandås, B.T.G., et al., eds., Onshore-offshore relationships on the North Atlantic Margin: Proceedings of a conference held in Trondheim, 2002: Norwegian Petroleum Society (NPF) Special Publication 12: Amsterdam, Elsevier.

Brown, H., Holbrook, W., Hornbach, M., and Nealon, J., 2006, Slide structure and role of gas hydrate at the northern boundary of the Storegga Slide, offshore Norway: Marine Geology, v. 229, p. 179–186, doi: 10.1016/j.margeo.2006.03.011.

Davis, E., and Hyndman, R.D., 1989, Accretion and recent deformation of sediments along the northern Cascadia subduction zone: Geological Society of America Bulletin, v. 101, p. 1465–1480, doi:10.1130/0016-7606(1989)101<1465:AARDOS>2.3.CO;2.

Dillon, W., Danforth, W., Hutchinson, D., Drury, R., Taylor, M., and Booth, J., 1998, Evidence for faulting related to dissociation of gas hydrate and release of methane off the southeastern United States, *in* Henriet, J.P., and Mienert, J., eds., Gas hydrates: Relevance to world margin stability and climate change: Geological Society of London Special Publication 137, p. 293–302.

Goldfinger, C., Nelson, C.H., Johnson, J.E., and the Shipboard Scientific Party, 2003, Holocene earthquake records from the Cascadia subduction zone and northern San Andreas fault based on precise dating of offshore turbidites: Annual Review of Earth and Planetary Sciences, v. 31, p. 555–577, doi: 10.1146/annurev.earth.31.100901.141246.

Hornbach, M., Lavier, L., and Ruppel, C., 2007, Triggering mechanism and tsunamogenic potential of the Cape Fear Slide complex, U.S. Atlantic margin: Geochemistry Geophysics Geosystems, v. 8, Q12008, doi: 10.1029/2007GC001722.

Hyndman, R., Rogers, G., Dragert, H., Wang, K., Clague, J., Adams, J., and Bobrowsy, P., 1996, Giant earthquakes beneath Canada's west coast: Geoscience Canada, v. 23, p. 63–72.

Kvalstad, T., Andersen, L., Forsberg, C., Berg, K., Bryn, P., and Wangen, M., 2005, The Storegga slide: Evaluation of triggering sources and slide mechanics: Marine and Petroleum Geology, v. 22, p. 245–256, doi: 10.1016/j.marpetgeo.2004.10.019.

López, C.D., 2008, Seismic velocity structure associated with gas hydrate at the frontal ridge of northern Cascadia margin [M.S. thesis]: Victoria, Canada, University of Victoria, 145 p.

Mienert, J., Vanneste, M., Bünz, S., Andreassen, K., Haflidason, H., and Sejrup, H., 2005, Ocean warming and gas hydrate stability on the mid-Norwegian margin at the Storegga Slide: Marine and Petroleum Geology, v. 22, p. 233–244, doi: 10.1016/j.marpetgeo.2004.10.018.

Mosher, D., 2009, International year of planet Earth 7. Oceans: Submarine landslides and consequent tsunamis in Canada: Geoscience Canada, v. 36, p. 179–190.

Pecher, I., Henrys, S., Ellis, S., Chiswell, S., and Kukowski, N., 2005, Erosion of the seafloor at the top of the gas hydrate stability zone on the Hikurangi Margin, New Zealand: Geophysical Research Letters, v. 32, L24603, doi: 10.1029/2005GL024687.

Pohlman, J., Riedel, M., Waite, W., Rose, K., Lapham, L., Hamilton, T., Enkin, R., Spence, G., Hyndman, R., and Haacke, R., 2008, Geochemical investigation of slope failure on the northern Cascadia margin frontal ridge: Eos (Transactions, American Geophysical Union) v. 89, Fall meeting supplement, abs.OS32A–08.

Riedel, M., Collett, T., Malone, M., and the Expedition 311 Scientists, 2006, Proceedings of the Integrated Ocean Drilling Program, Volume 311: Washington, D.C., Integrated Ocean Drilling Program Management International, Inc., doi: 10.2204/iodp.proc.311.2006.

Solheim, A., Forsberg, C., and Bryn, P., 2005, The Storegga Slide complex: Repetitive large scale sliding with similar cause and development: Marine and Petroleum Geology, v. 22, p. 97–107, doi: 10.1016/j.marpetgeo.2004.10.013.

Synolakis, C., Bardet, J.-P., Borrero, J., Davies, H., Okal, E., Silver, E., Sweet, S., and Tappin, D., 2002, The slump origin of the 1998 Papua New Guinea tsunami: Royal Society of London Proceedings, ser. A, v. 458, p. 763–789, doi: 10.1098/rspa.2001.0915.

Wright, S., and Rathje, E., 2003, Triggering mechanisms of slope instability and their relationship to earthquakes and tsunamis: Pure and Applied Geophysics, v. 160, p. 1865–1877, doi: 10.1007/s00024-003-2410-4.

Manuscript received 19 February 2010
Revised manuscript received 8 June 2010
Manuscript accepted 11 June 2010

Printed in USA